# Detergent Properties Influence the Stability of the Glycophorin A Transmembrane Helix Dimer in Lysophosphatidylcholine Micelles

Michael Stangl,[†] Anbazhagan Veerappan,[†‡] Anja Kroeger,[§] Peter Vogel,[†] and Dirk Schneider[†*]
[†]Institut für Pharmazie und Biochemie, Johannes Gutenberg-Universität Mainz, Mainz, Germany; [‡]School of Chemical and Biotechnology, SASTRA University, Thanjavur, Tamil Nadu, India; and [§]Max Planck Institute for Polymer Research, Mainz, Germany

ABSTRACT Detergents might affect membrane protein structures by promoting intramolecular interactions that are different from those found in native membrane bilayers, and fine-tuning detergent properties can be crucial for obtaining structural information of intact and functional transmembrane proteins. To systematically investigate the influence of the detergent concentration and acyl-chain length on the stability of a transmembrane protein structure, the stability of the human glycophorin A transmembrane helix dimer has been analyzed in lyso-phosphatidylcholine micelles of different acyl-chain length. While our results indicate that the transmembrane protein is destabilized in detergents with increasing chain-length, the diameter of the hydrophobic micelle core was found to be less crucial. Thus, hydrophobic mismatch appears to be less important in detergent micelles than in lipid bilayers and individual detergent molecules appear to be able to stretch within a micelle to match the hydrophobic thickness of the peptide. However, the stability of the GpA TM helix dimer linearly depends on the aggregation number of the lyso-PC detergents, indicating that not only is the chemistry of the detergent headgroup and acyl-chain region central for classifying a detergent as harsh or mild, but the detergent aggregation number might also be important.

## INTRODUCTION

Because they mimic many aspects of cellular membranes, detergents are typically used for membrane protein extraction, purification and structural analyses, and for studies aiming to analyze the energetics of transmembrane (TM) protein folding and stability. Detergents not only provide a hydrophobic environment (thereby stabilizing a protein structure), they also serve as an intimate solvent and impose numerous restrictions on TM protein folding, assembly, and stability. When detergent molecules bind only to the formally lipid-exposed TM protein surface area, but not at sites of protein-protein contacts, the detergent molecules might simply replace bilayer lipids and the structural integrity of a TM protein will be preserved. Indeed, several experiments have shown that secondary and tertiary structure elements may be similar in a micellar environment and in lipid bilayers (1), and even a native protein quaternary structure may be maintained in detergents (2,3). Thus, the overall fold and structure of a TM protein can be preserved in a detergent environment.

However, detergents can also affect TM protein structures by promoting intramolecular interactions different from those found in native membrane bilayers (4,5). For example, bacteriorhodopsin crystallized as a monomer in a bicellar environment, whereas in the lipid cubic phase it crystallized as a trimer (6–8). While it was previously assumed that the *Escherichia coli* diacylglycerol kinase requires lipid cofactors, recent studies have indicated that the protein can sustain its native structure, stability, and activity in a defined lipid-free detergent (9). Thus, selecting proper detergent conditions can be crucial to preserve a correct protein structure and function. However, the ability of some (if not all) detergents to preserve the native structure and function of a TM protein appears to differ on a case-by-case basis. Therefore, determination of the detergent and buffer conditions necessary to maintain the structure and function of a TM protein upon solubilization is still an empirical and frequently time-consuming process.

Interactions of detergents with TM proteins depend on the protein itself, such as the TM amino-acid sequence and the secondary structure propensity, as well as on the actual detergent concentration and on detergent properties, such as the headgroup chemistry, the length of acyl chain, or the micelle structures. Identifying a proper detergent used for TM protein solubilization and analyses may be guided by categorizing detergents into mild or harsh detergents, based on their propensity to preserve or disrupt a TM protein structure (10–12). The characteristics of longer tail length, larger detergent headgroup size, and neutral headgroup charge have been identified, in the main, as preservative of TM protein structures, and would therefore be used to classify a detergent as mild. However, the responses of membrane protein structures to detergent solubilization still cannot be safely predicted. Luckily, the range of detergents available for membrane protein research has increased significantly in recent years, now allowing us to find a proper detergent for gaining deeper insight into structure-function relationship of membrane proteins or in the principle guiding membrane protein folding (11).

Although our understanding of the principles guiding membrane protein folding has significantly improved in recent years, the forces governing protein folding inside lipid bilayers are still poorly understood (13,14). Two

*Submitted March 8, 2012, and accepted for publication November 5, 2012.*

*Correspondence: dirk.schneider@uni-mainz.de

Editor: William Wimley.



0006-3495/12/12/2455/10 $2.00

http://dx.doi.org/10.1016/j.bpj.2012.11.004

decades ago, the folding of $\alpha$-helical membrane proteins was simplified as a two-stage process: Stage 1, in which individual helices insert independently into the membrane; and Stage 2, in which these helices subsequently interact to form higher-ordered oligomeric structures (15). While this two-stage model significantly simplifies the problem of $\alpha$-helical membrane protein folding, it allows an uncomplicated but meaningful analysis of membrane protein folding, because formation of stable $\alpha$-helices and integration of helices into a membrane are uncoupled from the formation of a three-dimensional membrane protein structure. The human glycophorin A (GpA) TM helix dimer became a paradigm for studying the second stage of this two-stage process, as the TM region of GpA forms a stable, noncovalent helix dimer. The NMR structure of the GpA TM in DPC micelles (16), along with a wealth of information on the sequence-specific dimerization (17–22), have made this system ideal for analyzing the energetics of TM helix-helix interactions in more detail.

The stability of the GpA TM dimer studied in model membrane systems has indicated that interactions between helices are modulated by lipid acyl-chain order, by hydrophobic matching between the peptide and lipid bilayer as well as by the lipid headgroup chemistry (23,24). Thus, the membrane environment significantly influences GpA TM helix dimerization. Furthermore, a micellar environment also significantly influences association and the stability of the GpA helix dimer (25–28). It has been suggested that GpA peptide association is mainly driven by enthalpic forces in micelles, whereas at high detergent concentrations, peptide association is opposed by entropic forces (26).

Increasing detergent concentrations increase the number of available micelles, and thus of the effective solvent of the TM protein, which might result in dilution of the GpA dimer. While the thermodynamics underlying destabilization of the TM helix dimer have been well described for the influence of the headgroup chemistry, the impact of the acyl chain on the thermodynamics of a TM helix structure have been far less elucidated yet (26). The actual concentration of detergent monomers per micelle, the aggregation number, might also affect the stability of a TM helix-helix interaction—an aspect not yet considered. Furthermore, it is still a matter of debate whether the radius of the hydrophobic micelle core affects the stability of a TM structure (i.e., whether hydrophobic match/mismatch determines the stability of a TM structure in a detergent micelle (12,29)).

In this study, we analyzed the stability of the GpA TM helix dimer in detergent micelles. We used lyso-phosphatidylcholine (lyso-PC) micelles of different acyl-chain length to systematically investigate the influence of the detergent concentration and acyl-chain length on the stability of a TM structure, excluding any effects caused by the detergent headgroup chemistry or by introducing mutations into the peptide. Furthermore, we analyzed the influence of the detergent aggregation number as well as that of the micelle's hydrodynamic radius on the stability of a TM structure. Based on our results, dissociation of the GpA TM helix dimer cannot be explained by simple dilution, because, in addition to the detergent concentration, direct protein-detergent interactions or detergent properties (such as the acyl-chain hydrophobicity and the detergent aggregation number) might influence the stability of the $\alpha$-helical TM protein. Importantly, the GpA TM helix dimer was found to not be most stable when the measured hydrodynamic radius of the micelle matches the hydrophobic region of the TM helix dimer. Consequently, the concept of hydrophobic match/mismatch cannot be easily transferred from membrane systems to detergent environments—at least, not for lyso-PC detergents.

## MATERIALS AND METHODS

### Materials

Peptides corresponding to residues 69–101 of the human GpA TM domain (SEPEITLIIFGVMAGVIGTILLISYGIRRLIKK) were custom-synthesized and labeled at the N-terminus with the donor and acceptor dyes fluorescein (Fl) and 5-6-carboxyrhodamine (TAMRA), respectively (Peptide Specialty Laboratories, Heidelberg, Germany). The purity of the peptides was confirmed by HPLC and mass spectrometry. Peptides were dissolved in 2,2,2-trifluoroethanol purchased from Sigma-Aldrich (Munich, Germany). Lyso-PC detergents C10–C16 were purchased from Avanti Polar Lipids (Alabaster, AL) and dissolved in chloroform/methanol (2:1).

### FRET measurements

For FRET measurements, equal concentrations (1:1 mol ratio) of Fl- and TAMRA-labeled GpA TM domains were used. The concentrations of the peptide stock solutions were determined from absorbance measurements in a Lambda 35 UV/Vis spectrophotometer (PerkinElmer, Boston, MA). In all experiments, we used 0.25 $\mu$M for each labeled GpA peptide. Peptides, dissolved in trifluoroethanol and detergent, dissolved in chloroform/methanol (2:1), were mixed and organic solvents were removed in a gentle stream of nitrogen gas. Final traces of the solvents were removed by vacuum desiccation overnight. The dried peptide-detergent film was hydrated in 10 mM HEPES buffer (pH 7.4) containing 150 mM NaCl.

After five freeze-thaw cycles, steady-state fluorescence measurements were performed at 25°C in a Spectronic Bowman series-2 luminescent spectrometer (Thermo Scientific, Waltham, MA) having both the excitation and the emission bandpass filter set at 4 nm. The excitation wavelength was 439 nm and emission spectra were recorded from 480 to 650 nm.

To follow the effect of the detergent environment and increasing detergent concentrations on a defined TM helix-helix interaction, we studied the dissociation of the GpA TM helix dimer following the EmEx-FRET method (30,31), which allows determining the concentration of GpA TM helix dimers in micelles.

Energy transfer $E$ was calculated using the donor fluorescence intensities at 525 nm in the presence and absence of acceptor according to

$$E = 1 - \left(\frac{F_{DA}}{F_D}\right). \quad (1)$$

$F_D$ is the fluorescence intensity of the donor sample and $F_{DA}$ is the fluorescence intensity of the sample containing donor and acceptor GpA TM

domain at equal concentrations. The energy transfer of sequence-specific TM helix dimerization, $E_D$, can be expressed as

$$E_D = f_D P_D E_R, \quad (2)$$

where $f_D$ is the fraction of dimeric TM helices, $P_D$ is the probability for donor quenching when the peptides form a dimer, and $E_R$ is the energy transfer in the dimer.

The probability $P_D$ for donor quenching depends on the molar ratio of the acceptor peptides $\chi_a$ = [a]/([a]+[d]), where [a] and [d] are the concentrations of the acceptor and donor peptides, respectively. The distance of the fluorophores in the GpA helix dimer is much smaller than the Förster radius, and thus $E_R$ can be set as 1.

The fraction dimer, $f_D$, can be written as $f_D = 2[D]/[T]$, where [D] is the concentration of dimeric peptides and [T] the total peptide concentration. Therefore, the dimer concentration [D] can be calculated by

$$[D] = \frac{E_D[T]}{2\chi_a}. \quad (3)$$

The dissociation constant, $K_D$, and the corresponding standard Gibbs free-energy change of dissociation, $\Delta G^{\circ}$, are given by

$$K_D = \frac{[M]^2}{[D]}, \quad (4)$$

$$\Delta G_D^0 = -RT \ln K_D, \quad (5)$$

where the monomer concentration is [M] = [T] – 2[D].

## Circular dichroism

Circular dichroism (CD) spectra were recorded on a J-815 spectropolarimeter (JASCO, Easton, MD) at 25°C with a scan speed of 100 nm/min using 0.1-cm-pathlength quartz cells from Hellma (Mühlheim, Germany). The concentration of unlabeled GpA peptide was 18 $\mu$M. Data points were collected with a resolution of 1 nm, an integration time of 1 s, and a slit width of 1 nm. Each spectrum shown is the result of at least three averaged consecutive scans, from which buffer scans were subtracted. The measured ellipticity $\theta$ (deg) was converted to molar ellipticity by

$$\text{Molar ellipticity} = 100\left(\frac{\theta}{L\,C}\right), \quad (6)$$

where $L$ is the path length and $C$ is the peptide concentration.

The GpA TM domain has been mixed in organic solvent with 20 mM lyso-PCs having acyl-chain lengths ranging from C10 to C16. After removal of the organic solvents by nitrogen and desiccation, samples were hydrated with 50 mM phosphate buffer pH 7.4. Before measuring, samples were treated identically as for the FRET measurements. The secondary structure contents were predicted using the software package DICHROWEB (http://dichroweb.cryst.bbk.ac.uk/html/home.shtml), which contains both soluble and TM proteins as a reference data set (32,33).

## Critical micellar concentration and aggregation number $N_{agg}$ determination by fluorescence spectroscopy

The critical micellar concentration (cmc) of each lyso-PC was determined by following 1-anilinonaphtalene-8-sulfonate fluorescence (34). A detergent stock solution (concentration 20- to 40-fold above the expected cmc) was titrated in 10 mM HEPES buffer containing 150 NaCl, 5 $\mu$M 1-anilinonaphtalene-8-sulfonate, pH 7.4. After each addition, a fluorescence spectrum was monitored from 450 to 600 nm after excitation at 374 nm. The fluorescence intensity at 490 nm was then plotted as a function of the detergent concentration, and the cmc was evaluated by linear least-squares fitting. Data points before and after the change of the slope were fitted to two straight lines. The cmc values were determined by the intersection of the two straight lines using at least two independent measurements. The $R^2$ coefficient of determination was always above 0.95 for the fitted straight lines, hence potential errors caused by fitting were neglectable.

The number of molecules forming micelles (aggregation number $N_{agg}$) was determined by a fluorescence quenching method as described in detail in the literature (35,36). Briefly, 2 $\mu$M of pyrene dissolved in 20 mM lyso-PC was quenched with *n*,*n*-dibutyl aniline (concentration range varied from 0 to 100 $\mu$M) and the fluorescence intensity at 373 nm was measured (excitation at 337 nm). The aggregation number $N_{agg}$ was calculated by

$$N_{agg} = \frac{([D_c] - cmc)}{[M_c]}, \quad (7)$$

where $D_c$, $cmc$, and $M_c$ represent the total detergent concentration, the critical micellar concentration, and the actual concentration of micelles, respectively. The unknown parameter, $M_c$, was determined by

$$\ln\left(\frac{I_0}{I}\right) = \frac{[Q]}{[M_c]}, \quad (8)$$

where $I_0$ and $I$ are the fluorescence intensity of pyrene before and after addition of *n*,*n*-dibutyl aniline, respectively, and $[Q]$ is the quencher concentration. A plot of $\ln(I_0/I)$ versus $[Q]$ was fitted with a straight line with a slope of $1/M_c$. Aggregation numbers $N_{agg}$ can be then calculated using Eq. 7.

## Light scattering

Static-light-scattering (SLS) and dynamic-light-scattering (DLS) experiments were performed on an instrument consisting of a goniometer and an ALV-5004 multiple-tau full-digital correlator (320 channels; ALV, Langen/Hessen, Germany), which allows measurements over a time range $10^{-7} \le t \le 10^3$ s and an angular range from 30° to 150° corresponding to a scattering vector $q = 6.9 \times 10^{-3} - 2.6 \times 10^{-2}$ nm$^{-1}$. An He-Ne laser (with a single mode intensity of 25 mW operating at a laser wavelength of $\lambda_0$ = 632.8 nm; JDS Uniphase, Milpitas, CA) was used as a light source. Dust-free samples for SLS and DLS experiments were obtained by filtration through PTFE membrane filters with a pore-size of 5 $\mu$m (LCR syringe filters; Millipore, Billerica, MA) directly into cylindrical silica-glass cuvettes (inner diameter Ø = 20 mm; Hellma) that had been cleaned with acetone in a Thurmont-apparatus. The cuvettes containing the sample solutions were placed into a thermostated refractive index-matching toluene bath held at a constant temperature of $T$ = 25°C.

In the SLS experiments, the reduced absolute intensity ratio $R(q)/(Kc)$ at a concentration $c$ was computed from the Rayleigh ratio $R(q)$,

$$R(q) = \frac{I(q)_{so\ln} - I(q)_{solv}}{I(q)_t}\left(\frac{n_{solv}}{n_t}\right)^2 R_t, \quad (9)$$

and the optical constant $K = (2\pi \cdot n\ dn/dc)^2/(\lambda_0^4 \cdot N_A)$; $I_{soln}$, $I_{solv}$, and $I_t$ are the light-scattering intensities of the solution, solvent, and the pure toluene, respectively. Toluene was used as a standard with refractive index $n_t$ and Rayleigh ratio $R_t = 2.2 \cdot 10^{-5}$ cm$^{-1}$. $N_A$ is the Avogadro number.

The refractive index increment $dn/dc = 0.1359$ mL g$^{-1}$ was determined at $\lambda$ = 633 nm using a scanning Michelson interferometer. Further theoretical details of the DLS experiments and specifics of the data evaluation by using the constraint-regularized CONTIN method are given elsewhere (37).

## RESULTS

### GpA TM helix secondary structure in lyso-PCs

The impact of detergent properties on the stability of the GpA TM helix dimer was systematically analyzed in lyso-PC micelles, having acyl-chain lengths ranging from C10 to C16. To ensure that the secondary structure of the GpA TM helix was preserved in the respective lyso-PC micelles, far-UV CD spectra of the GpA TM peptide were recorded in the various lyso-PCs (Fig. 1). In all tested detergents, the TM domain showed characteristics typical for an $\alpha$-helical structure with a maximum at ~193 nm and double-minima at 208 nm and 222 nm. Calculation of the secondary structure using the software package DICHROWEB suggested an $\alpha$-helix content between 78 and 81% for most tested lyso-PCs at a detergent concentration of 20 mM (Table 1). Of note, the $\alpha$-helix content of the peptides did not depend on the actual lyso-PC concentrations. While the CD data clearly demonstrates that the secondary structure of the GpA TM domain is well preserved in the tested lyso-PCs, it is impossible to determine the fractions of monomeric or dimeric GpA solely by CD, as the peptides have essentially identical CD spectra. Such identical CD spectra of both monomeric and dimeric GpA in detergents have been previously reported (25,27). Therefore, to analyze the stability of the TM helix dimer in lyso-PC micelles, we performed FRET measurements.

### The stability of the GpA TM domain dimer depends on the lyso-PC acyl-chain length

To quantitatively analyze the influence of defined lyso-PC properties on a TM helix dimer stability, we monitored GpA TM helix dimerization in lyso-PCs with different acyl-chain lengths by fluorescence spectroscopy. In Fig. S1 in the Supporting Material, we show fluorescence excitation and emission spectra of Fl- and TAMRA-labeled GpA peptides. The Fl emission spectrum overlaps significantly with the TAMRA excitation spectrum. The distance between the amino termini of the GpA TM helices in the dimer, as calculated from the NMR structure, is ~10 Å, which is far below the Förster radius ($R_0$) of the Fl/TAMRA FRET pair (49–54 Å) (38). Thus, the energy transfer measured as donor emission quenching and/or sensitized acceptor emission (see Fig. S1 *C*) is a direct measure of GpA TM helix dimerization.

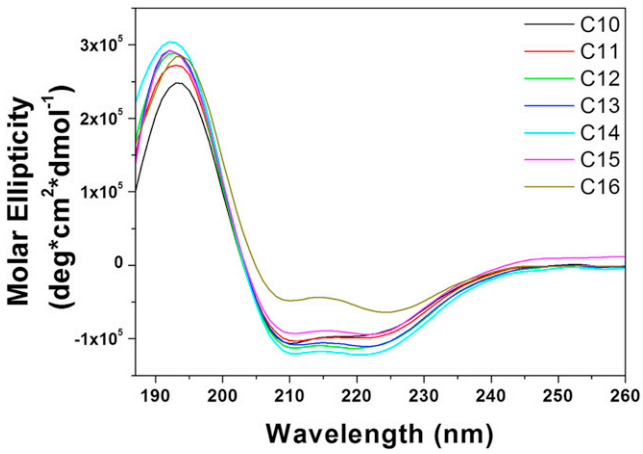


FIGURE 1 Far UV-CD spectra of the GpA TM domain in 20 mM lyso-PCs. C10-lysoPC (*black*), C11-lysoPC (*red*), C12-lysoPC (*green*), C13-lysoPC (*blue*), C14-lysoPC (*cyan*), C15-lysoPC (*magenta*), and C16-lysoPC (*yellow*). The measured ellipticities were converted to molar ellipticity as described in Materials and Methods.

**TABLE 1 Helical content of the GpA TM domain in 20 mM lyso-PCs with increasing acyl-chain lengths as determined by the program DICHROWEB**

| Lyso-PC | $\alpha$-helical content [%] |
|---|---|
| 10 | 81 |
| 11 | 81 |
| 12 | 79 |
| 13 | 78 |
| 14 | 78 |
| 15 | 78 |
| 16 | 66 |

FRET measurements were performed in presence of 20 mM lyso-PCs having increasing acyl-chain length, and the normalized emission spectra of the FRET pair are shown in Fig. 2 *A*. The sensitized emission at 575 nm decreased with increasing acyl-chain length, indicating a decreasing stability of the GpA TM helix dimer. The individual GpA dimer fractions in the various lyso-PCs, as calculated from the donor and FRET pair emission spectra (Fig. 2 *B*), strongly suggest a correlation between the acyl-chain length and the stability of the dimer, with the highest dimer fraction of ~60 % observed in C10 lyso-PC. The stability of the dimer decreases with increasing lyso-PC acyl-chain lengths (Fig. 2), most likely because hydrophobic interactions of the lyso-PCs with the GpA TM helix increase with increasing lyso-PC acyl-chain lengths.

Together, our results suggest that the GpA TM domain forms a stable dimer in all analyzed lyso-PCs and that the lyso-PC acyl-chain length affects the dimerization propensity in micelles.

### The stability of the GpA TM domain dimer depends on the lyso-PC concentration

To analyze the influence of the various lyso-PC detergents on the energetics of the TM helix-helix interaction in more detail, we then measured the thermodynamic stability of the GpA TM helix dimer at different lyso-PC concentrations.

Concentration-dependent dimerization of the GpA TM domain in lyso-PC micelles was studied by monitoring resonance energy transfer with fluorescently labeled GpA TM peptides. All experiments were performed at a constant peptide concentration by varying only the lyso-PC

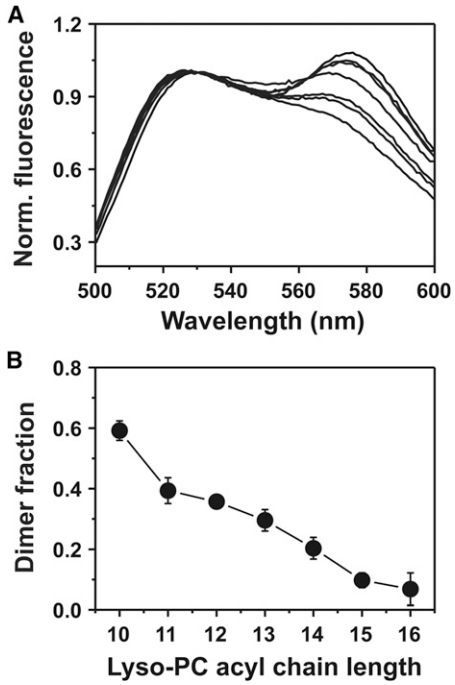


FIGURE 2 Self-association of GpA peptides in 20 mM lyso-PCs. Fluorescence emission was measured in micelles with Fl-labeled peptide alone as well as with the Fl- and TAMRA-labeled peptide pair (1:1 ratio). Energy transfer was calculated from the Fl-fluorescence decrease at 525 nm. (*A*) FRET spectra recorded for Fl- and TAMRA-labeled peptides dissolved in 20 mM $C_n$ lyso-PC detergents. (*Upper spectrum*) This data originates from peptides dissolved in C10-lyso PC micelles and the others were measured in lyso-PCs having increasing acyl-chain lengths (C10–C16), resulting in decreasing energy transfer. (*B*) Fraction dimer plotted against the acyl-chain length of the various lyso-PCs.

concentrations. The inset in Fig. 3 *A* shows representative emission spectra of the FRET pair (1:1 ratio) at increasing lyso-PC concentrations. The relative decrease in the sensitized emission at 575 nm with increasing lyso-PC concentration clearly indicates destabilization of the GpA TM helix dimer. The dimer fractions at increasing detergent concentrations, as calculated from the measurements shown in the inset, are summarized in Fig. 3 *A* for C10 and C16 lyso-PCs. Irrespective of the acyl-chain length, the fraction of dimeric GpA, and thus the stability of the GpA TM helix-helix interaction, decreases nonlinearly with increasing detergent concentrations. Thus, with increasing detergent concentrations, the GpA TM monomer-dimer equilibrium significantly shifts toward the monomer in all analyzed lyso-PCs. Based on measurements as shown in Fig. 3 *A*, the apparent GpA dissociation constants were calculated in the various lyso-PC detergents at increasing concentrations (see Table S1 in the Supporting Material). Fig. 3 *B* shows the apparent $K_D$ values calculated based on the FRET measurements performed in C10 and C16 lyso-PC. All calculated $K_D$ values are summarized in Table S1.

While the stability of the GpA TM helix dimer appears to depend on the lyso-PC acyl-chain length, the observed

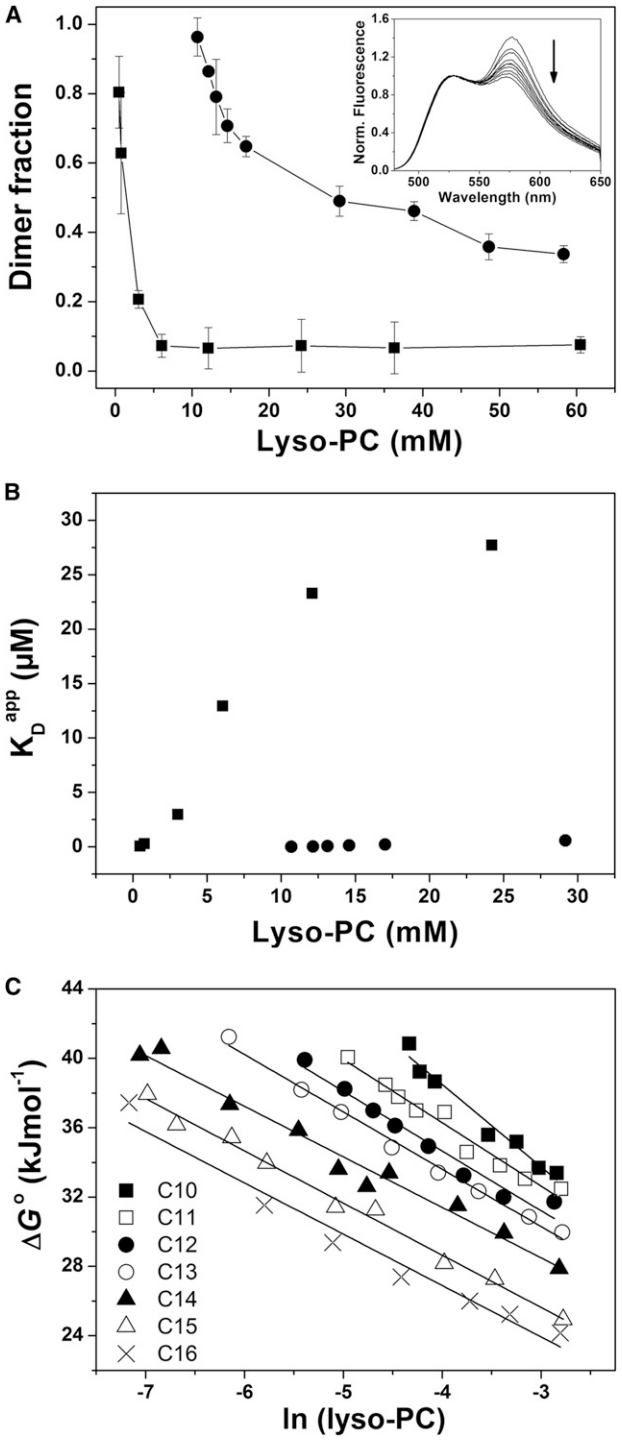


FIGURE 3 Concentration-dependent dimerization of the GpA TM domain. (*A*) GpA TM helix dimer fractions calculated from FRET spectra obtained at various C10 (●) and C16 (■) lyso-PC concentrations. The lyso-PC concentrations are given on the *x* axis. (*Inset*) FRET spectra recorded for Fl- and TAMRA-labeled peptides (1:1 mol ratio) in C10 lyso-PC micelles. All spectra were normalized at 525 nm. (*Arrow*) Spectral shifts at increasing C10 lyso-PC concentrations. (*B*) Apparent GpA TM dissociation constant determined in C10 (●) and C16 (■) lyso-PC micelles at increasing detergent concentrations. (*C*) Apparent dissociation free energy values ($\Delta G^\circ$) calculated from the apparent $K_D$ values shown in panel *A* and summarized in Table S1.

dimerization propensities at a given detergent concentration might not be compared directly, because detergent properties, such as the critical micellar concentration (cmc) or aggregation number of the respective lyso-PCs, vary with increasing acyl-chain length. Thus, we next determined the cmc as well as aggregation numbers of lyso-PC micelles (Table 2). In Fig. S2, the cmc values of the analyzed lyso-PCs are summarized, and the cmc values decrease exponentially with increasing acyl-chain length. The mean aggregation number, $N_{agg}$, was determined at 20 mM lyso-PC by a pyrene fluorescence-quenching method as described in Materials and Methods (Fig. 4 *A*). To rule out any potential interference from pyrene eximer formation during the fluorescence $N_{agg}$ determination, we additionally measured the pyrene fluorescence from 360 to 500 nm at varying lyso-PC concentrations (see Fig. S3). Because no peak at 480 nm was observed, pyrene eximer formation could be excluded, confirming that the observed fluorescence quenching was only caused by addition of the quencher (*n*,*n*-dibutyl aniline).

The aggregation numbers $N_{agg}$ of lyso PC samples having acyl-chain lengths of C10–C16 were additionally confirmed by light-scattering measurements (Fig. 4 *A*). The apparent weight-average molar masses $M_{Wapp}$ of the resulting supramolecular assemblies (micelles) were obtained from Ornstein-Zernicke plots ($Kc/R_{VV}$ ($q$) versus $q^2$), as shown in Fig. 5. The intercept of an extrapolation $q \rightarrow 0$ in the linear regime for each sample yields values of $M_{Wapp} = (1.63 \pm 0.2) \times 10^4$ g mol$^{-1}$ for C10 to $M_{Wapp} = (1.03 \pm 0.1)\ 10^5$ g mol$^{-1}$ for C16, which results in $N_{agg}$ between 40 and 209, respectively (Table 2). Fig. 4 *A* shows the lyso-PC aggregation numbers as a function of the acyl-chain length determined by fluorescence quenching (*solid circles*), which is supported by the data obtained from light-scattering experiments (*open circles*). While at higher acyl-chain lengths the aggregation numbers determined by the fluorescence method differ from the values obtained by light scattering, the aggregation numbers nearly increase linearly with increasing acyl-chain length of the lyso-PCs (Fig. 4 *A*), as demonstrated by both applied methods.

The $N_{agg}$ values determined by the two techniques vary from 35/47 for C10 lyso-PC to 112 for C16 lyso-PC when determined by the fluorescence technique, or to 209 for C16 lyso-PC when determined by light scattering. As of this writing, there are only a few lyso-PC aggregation numbers available from the literature. For C10 and C12 lyso-PCs, we determined aggregation numbers of 35/40 and 78/82 at a detergent concentration of 20 mM (Table 2), which are in good agreement with values determined by NMR spectroscopy (34 for C10 and 55 for C12 lyso-PC) (39).

Beyond the aggregation numbers of the micelles, the corresponding micelle sizes were determined by DLS experiments and summarized in Table 2 as $z$-average hydrodynamic radii $R_h$. The $R_h$ values are in the range of 24–37 Å, and increase linearly with increasing lyso-PC acyl-chain length (Fig. 4 *B* and Table 2).

## Sequence specificity of GpA TM helix dimerization in lyso PC micelles

To rule out that the results presented in Figs. 2 and 3 and Table S1 are influenced by unspecific aggregation of the TM peptides or by formation of higher-ordered oligomeric structures, formation of a sequence-specific GpA TM helix dimer was analyzed by monitoring energy transfer at constant peptide and detergent concentrations as a function of the donor/acceptor ratio, as reported in the literature (23,40). Fig. 6 shows FRET efficiencies as a function of the acceptor mole ratio in C14 lyso-PC micelles at 1 mM total detergent concentration. As discussed in detail in the literature (25,40), linear dependence of the FRET efficiency on the acceptor mole ratio indicates, exclusively, dimer formation. This control has also been performed in lyso-PCs with increased acyl-chain length at different concentrations (data not shown) and a linear dependence of the FRET efficiency has always been observed.

Thus, we conclude that the observed FRET efficiencies directly measure formation of a dimeric GpA TM helix structure. Nevertheless, the measured FRET signal can have different origins. While on the one hand it originates from so-called real dimer formation, it might also be influenced by simple proximity effects. Because we used very low peptide/detergent molar ratios, ranging from 1:200 to 1:120,000 (see Table S1), proximity effects are very unlikely. However, to exclude proximity effects, we performed

**TABLE 2 Characteristics of lyso-PC micelles and the stability of the GpA TM helix dimer in different acyl-chain length lyso-PCs**

| Lyso-PC | Cmc (mM) | $M_{Wapp}$ ($10^4$ gmol$^{-1}$) | $R_h$ (Å) | $N_{agg}$ SLS | $N_{agg}$ Fluor. | $\Delta G^\circ_d$ (20 mM) (kJmol$^{-1}$) | $d\Delta G^\circ_d/d$ln(lyso-PC) (kJmol$^{-1}$) |
|---|---|---|---|---|---|---|---|
| C10 | 6.06 (6.0–8.0) | 1.63 | 24 | 40 | 35 | 38.12 ± 0.48 | −4.75 ± 0.37 |
| C11 | 1.81 (—) | 3.55 | 26 | 67 | 58 | 34.61 ± 0.26 | −3.65 ± 0.25 |
| C12 | 0.57 (0.4–0.9) | 3.62 | 28 | 82 | 78 | 33.28 ± 0.52 | −3.45 ± 0.26 |
| C13 | 0.15 (—) | 4.45 | 30 | 98 | 91 | 32.34 ± 0.14 | −3.31 ± 0.11 |
| C14 | 0.04 (0.04–0.09) | 5.87 | 33 | 126 | 90 | 31.51 ± 0.11 | −2.92 ± 0.15 |
| C15 | 0.010 (—) | 8.80 | 34 | 183 | 100 | 28.38 ± 1.30 | −3.01 ± 0.11 |
| C16 | 0.004 (0.004–0.008) | 10.34 | 37 | 209 | 112 | 28.15 ± 1.44 | −2.96 ± 0.23 |

Values in parentheses were obtained from a commercial website (Avanti Polar Lipids, Alabaster, AL).

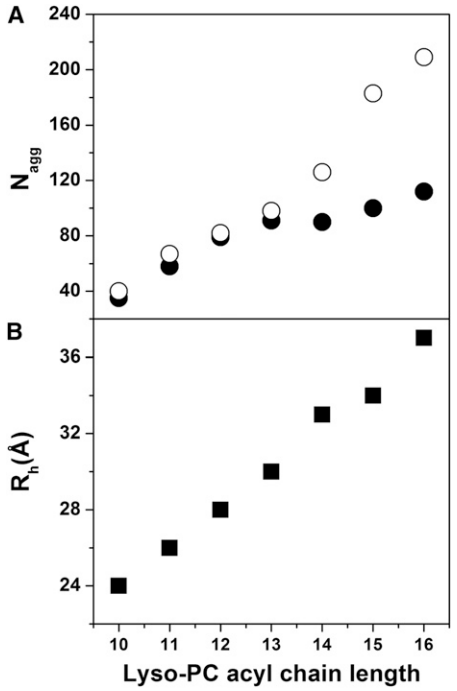


FIGURE 4 Aggregation numbers and hydrodynamic radii of lyso-PC micelles. (*A*) Mean aggregation number $N_{agg}$ as a function of the lyso-PC acyl-chain length at 20 mM detergent concentration determined by fluorescence quenching (●) and SLS (○). (*B*) Hydrodynamic radii $R_h$ of lyso-PC micelles determined by DLS.

FRET measurements upon addition of increasing concentrations of unlabeled GpA peptides, and observed a reduction in the FRET signal (Fig. 7). Upon addition of the unlabeled GpA TM peptides, the FRET signal decreases only if dimerization of the labeled peptides is sequence-specific (25,41).

Thus, the determined FRET efficiencies can be attributed to formation of a sequence-specific GpA TM helix dimer in lyso-PC micelles.

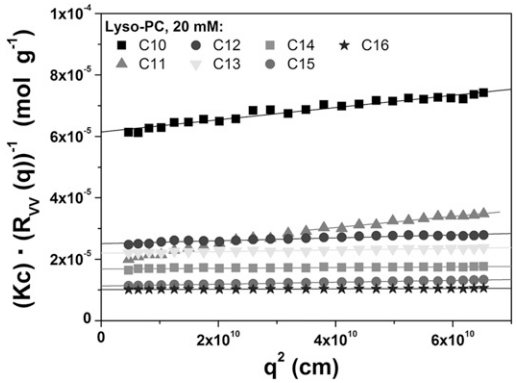


FIGURE 5 Static light-scattering analysis. Absolute light scattering intensity for the various lyso-PC at $c = 20$ mM in an Ornstein-Zernicke presentation for the determination of the molar masses using the intercept of an extrapolation ($q \rightarrow 0$) in the linear regime.

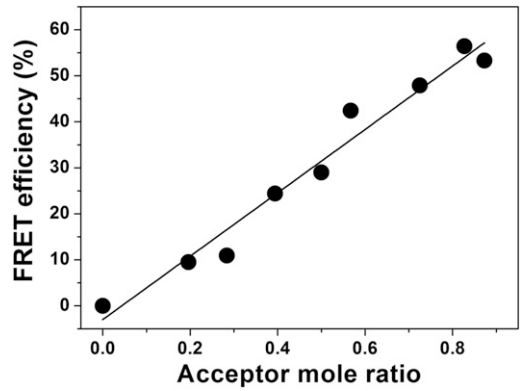


FIGURE 6 Stoichiometry of GpA association. FRET efficiencies as a function of acceptor mole fraction are shown for 1 mM C14 lyso-PC. The total peptide and detergent concentrations were kept constant, whereas the ratio of acceptor and donor peptide varied from 0.2 to 0.85. The linear dependence of the FRET efficiency on the acceptor mole ratio demonstrates exclusive dimer formation.

## DISCUSSION

Lysophosphatidylcholines (lyso-PCs) are naturally present in human cells and are released by spontaneous or enzymatic hydrolysis of PC lipids. Lyso-PCs are known to be

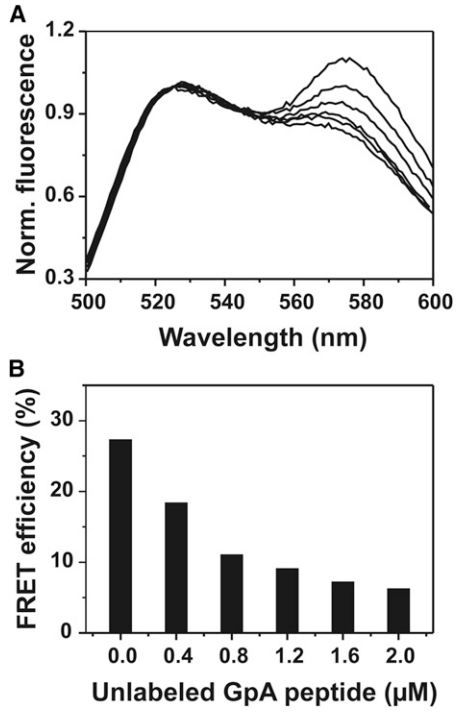


FIGURE 7 FRET competition assay. (*A*) FRET pair emission spectra in 5 mM C12 lyso-PC. Addition of 0.4–2 $\mu$M unlabeled GpA TM peptide (compare panel *A* with panel *B*) results in reduced sensitized acceptor emission. Spectra were normalized at 525 nm. (*Upper spectrum*) This data originates from peptides in the absence of unlabeled peptide. Stepwise addition of increasing amounts of unlabeled peptide results in decreased energy transfer, i.e., in decreased fluorescence emission at 575 nm. (*B*) FRET efficiencies calculated from the spectra shown in panel *A*.

involved in T-lymphocyte proliferation and protein kinase C activation (42,43), and the increased plasma lyso-PC concentration found in some cancer patients might be used as a marker for tumor progression (44,45). In vivo, most of the lyso-PC molecules are bound to albumins, which serve as a reservoir to rapidly provide lyso-PCs, if necessary, and eventually preserve membrane lysis (45,46). Because of their detergent properties, lyso-PCs form micellar structures and are membrane-lytic at high concentrations.

In our study, the impact of lyso-PC properties on a sequence-specific TM helix structure has been analyzed. By varying the acyl-chain length only and leaving the detergent headgroup chemistry identical, the influences of just the detergent acyl-chain on the stability of a TM structure have been systematically evaluated.

Thermodynamically, the free energy of helix-helix association in detergent micelles can be written as

$$\Delta G_a = \Delta G_{h-h} + n\Delta G_{d-d} - 2n\Delta G_{h-\mathrm{d}}, \qquad (10)$$

where $\Delta G_{h\text{-}h}$, $\Delta G_{d\text{-}d}$, and $\Delta G_{h\text{-}d}$ are the free energies of helix-helix, detergent-detergent, and helix-detergent interactions, respectively. It is assumed that formation of a helix-helix pair displaces $2n$ helix-detergent and results in $n$ gained detergent-detergent interactions. Dimerization of TM helices will be driven by a favorable value of $\Delta G_{h\text{-}h}$, arising, for example, from van der Waals' forces, salt-bridge, or hydrogen-bonding interactions between helices. Furthermore, rather weak interactions of the genetive headgroups with TM helices and poor packing of the acyl chains to the rough surface of TM helices might disfavor helix-detergent interactions and drive helix dimerization. However, interactions between the detergent acyl chains and the hydrophobic TM helix most likely increase with increasing acyl-chain length, which is coupled with increasing acyl-chain hydrophobicity, and consequently the free energies of dimerization decrease in lyso-PC micelles with increasing acyl-chain length (Fig. 3 *C* and Table 2). Notably, this observation contrasts with earlier findings in which it has been concluded that detergents with longer acyl-chain length generally tend to stabilize the structure of TM proteins (11).

However, irrespective of the genitive acyl-chain length, increasing detergent concentrations generally destabilize the GpA helix dimer (Fig. 3), as demonstrated by the increasing dissociation constants (Fig. 3 *B*, and see Table S1). This destabilization has been observed before and might be explained by a simple dilution effect based on entropically driven dissociation (26). In the ideal case, dissociation of helices caused by simple peptide dilution due to increasing detergent concentrations results in a slope of $-2.48$ kJ mol$^{-1}$ (8.314 J mol$^{-1}$ K$^{-1}$ $\times$ 298 K). However, while the calculated free energies of dissociation linearly depend on the lyso-PC concentration in all tested lyso-PCs (Fig. 3 *C*), the slopes vary from $-4.75$ to $-2.96$ kJmol$^{-1}$ (Table 2). Only dimerization in C16 lyso-PC is close to ideality and might be explained by simple dilution. Inconsistency from ideality, as usually observed, suggests a general mechanism driving helix-helix dissociation that is far more complex than simple dilution; and helix-detergent or detergent-detergent interactions, and the corresponding free energies, also eventually influence monomerization. Furthermore, because the properties of detergent micelles (such as the aggregation number or the hydrodynamic micelle radius) change with increasing acyl-chain length, the properties of the most intimate environment of a TM protein (the micelle it resides in) could also influence the stability of the TM helix oligomer. Thus, based on the results presented here, destabilization of a TM helix oligomer by increasing detergent concentration cannot be explained by simple dilution alone; a far more complex model is required.

In the past, several studies have shown that the structure of integral membrane proteins can highly depend on hydrophobic matching conditions, i.e., the thickness of the hydrophobic hydrocarbon core of the lipid bilayer must approximately match the hydrophobic region of the TM protein. Hydrophobic mismatch can result in severe destabilization of TM protein structures (47,48). Preservation of a TM protein structure in a lipid bilayer with changing bilayer thickness will alter lipid packing in the intimate surrounding bilayer, and the bilayer deformation energy is associated with local thickening or thinning of the lipid bilayer to match the hydrophobic region of the TM protein (49). Thus, it appears to be possible that a TM protein structure is most stable whenever the hydrophobic region of a micelle just about matches the hydrophobic region of a TM protein (29). On the other hand, detergent micelles are far more dynamic than lipid bilayers, and a micellar structure might adjust more easily to various TM protein structures (12). GpA dimerized in all tested lyso-PC micelles, and dimerization was most efficient in C10 lyso-PC but decreased with increasing lyso-PC acyl-chain length (Fig. 2 *B*, and see Table S1).

The observed high GpA TM helix dimerization propensity in C10 lyso-PC cannot be explained by simply considering the thickness of the hydrophobic micelle core, as the hydrophobic region of the GpA TM $\alpha$-helix dimer is ~31.3 $\pm$ 2.2 Å, whereas the diameter of the C10 lyso-PC micelles is only ~24 Å (Table 2). If the thickness of the hydrophobic micelle core were most important for stabilization of the GpA helix dimer (hydrophobic matching), the dimer should have been most stable in C13 or C14 lyso-PCs, having diameters of ~30 and 33 Å, respectively (Table 2). As this has not been observed, it appears to be rather likely that individual detergent molecules stretch within a micelle to match the hydrophobic thickness of the peptide. However, the structural dynamics of the micelle might be impaired when micelles are formed from detergents with

longer acyl chains, due to increased detergent-peptide and detergent-detergent interactions. Thus, with increasing acyl-chain length the elastic properties of the acyl chains decrease and eventually become insufficient to compensate a (potential) hydrophobic mismatch, resulting in destabilization of a TM protein structure. Notably, the $\alpha$-helical structure of the GpA TM domain, as determined by NMR in micelles (16) (PDB ID:1AFO and PDB ID:2KPE) and bicelles (50) (PDB ID:2KPF), was preserved in all analyzed lyso-PCs (Fig. 1).

Closer examination of the lyso-PC micelle properties over the range of the experimentally tested acyl-chain lengths also revealed that the lyso-PC aggregation numbers, $N_{agg}$, vary considerably for the various lyso-PCs (Fig. 4 *A*). The fraction dimeric GpA measured in 20 mM lyso-PCs with increasing acyl-chain length (Fig. 2) linearly correlates with the aggregation number of the respective detergent (Fig. 8). Because the concentration of detergent monomers per micelle, i.e., the peptide-to-detergent ratio per micelle, eventually influences the stability of a TM protein structure, this might indicate that the aggregation number can also affect the stability of the GpA TM helix dimer in a detergent micelle. With increasing $N_{agg}$, the number of detergent molecules per micelle (i.e., the concentration of the intimate solvent) is increased and the dimer fraction decreases, based on dilution and the law of mass action.

## CONCLUSION

Fine-tuning of detergent properties is crucial for obtaining structural information of intact and functional TM proteins. However, identifying a proper detergent suitable to maintain the structure, integrity, and function of a TM protein upon solubilization is still an empirical and time-consuming process.

Based on several previous studies of detergent properties and their impact on the stability of TM structures, some generalizing rules have emerged, classifying detergents as harsh or mild. However, the presented results indicate that the TM helix oligomer is destabilized in lyso-PCs with increasing chain length, which contrasts with the assumption that longer tails render detergents milder. Thus, the impact of the acyl-chain region on the stability of a TM structure appears to vary and one should be careful about generalizing the impact of an acyl-chain length on the structure and stability of a TM protein. Furthermore, individual detergent molecules appear to be able to stretch within a micelle to match the hydrophobic thickness of the peptide, and the diameter of the hydrophobic micelle core appears to be less important for selecting a proper detergent for structural and/or functional analyses, at least in case of lyso-PCs. Thus, hydrophobic mismatch might be less relevant in detergent micelles than in lipid bilayers.

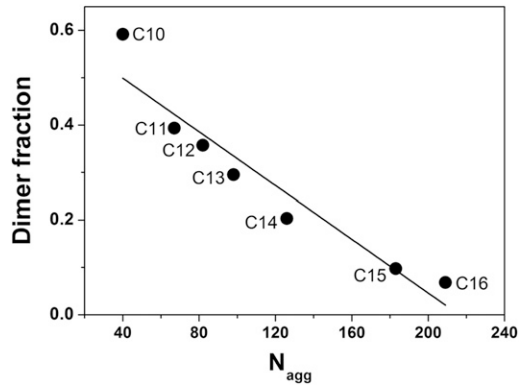


FIGURE 8 GpA stability and lyso-PC aggregation numbers. The fractions of dimeric GpA are plotted as a function of the lyso-PC aggregation number (different acyl-chain length) as determined by light scattering at 20-mM detergent concentration (compare to Fig. 5). The $N_{agg}$ value linearly correlates with the decrease of GpA TM domain dimer fraction with an $R^2$ of 0.9.

## SUPPORTING MATERIAL

One table and three figures are available at http://www.biophysj.org/biophysj/supplemental/S0006-3495(12)01225-8.

We thank H. Pearson for critically reading the manuscript. The authors thank Christine Rosenauer (Max Planck Institute for Polymer Research Mainz) for light-scattering experiments.

This work was supported by grants from the Deutsche Forschungsgemeinschaft, the Research Center for Complex Materials (COMATT), the University of Mainz, and the Max Planck Graduate Center with the University of Mainz.

## REFERENCES

1. Franzin, C. M., P. Teriete, and F. M. Marassi. 2007. Structural similarity of a membrane protein in micelles and membranes. *J. Am. Chem. Soc.* 129:8078–8079.
2. Veerappan, A., F. Cymer, …, D. Schneider. 2011. The tetrameric $\alpha$-helical membrane protein GlpF unfolds via a dimeric folding intermediate. *Biochemistry.* 50:10223–10230.
3. Melnyk, R. A., A. W. Partridge, and C. M. Deber. 2001. Retention of native-like oligomerization states in transmembrane segment peptides: application to the *Escherichia coli* aspartate receptor. *Biochemistry.* 40:11106–11113.
4. Federkeil, S. L., T. L. Winstone, …, R. J. Turner. 2003. Examination of EmrE conformational differences in various membrane mimetic environments. *Biochem. Cell Biol.* 81:61–70.
5. Chou, J. J., J. D. Kaufman, …, A. Bax. 2002. Micelle-induced curvature in a water-insoluble HIV-1 Env peptide revealed by NMR dipolar coupling measurement in stretched polyacrylamide gel. *J. Am. Chem. Soc.* 124:2450–2451.
6. Grigorieff, N., T. A. Ceska, …, R. Henderson. 1996. Electron-crystallographic refinement of the structure of bacteriorhodopsin. *J. Mol. Biol.* 259:393–421.
7. Faham, S., and J. U. Bowie. 2002. Bicelle crystallization: a new method for crystallizing membrane proteins yields a monomeric bacteriorhodopsin structure. *J. Mol. Biol.* 316:1–6.
8. Pebay-Peyroula, E., G. Rummel, …, E. M. Landau. 1997. X-ray structure of bacteriorhodopsin at 2.5 Ångstroms from microcrystals grown in lipidic cubic phases. *Science.* 277:1676–1681.
9. Koehler, J., E. S. Sulistijo, …, C. R. Sanders. 2010. Lysophospholipid micelles sustain the stability and catalytic activity of diacylglycerol kinase in the absence of lipids. *Biochemistry.* 49:7089–7099.

10. le Maire, M., P. Champeil, and J. V. Moller. 2000. Interaction of membrane proteins and lipids with solubilizing detergents. *Biochim. Biophys. Acta.* 1508:86–111.

11. Privé, G. G. 2007. Detergents for the stabilization and crystallization of membrane proteins. *Methods.* 41:388–397.

12. Therien, A. G., and C. M. Deber. 2002. Interhelical packing in detergent micelles. Folding of a cystic fibrosis transmembrane conductance regulator construct. *J. Biol. Chem.* 277:6067–6072.

13. Booth, P. J., and P. Curnow. 2009. Folding scene investigation: membrane proteins. *Curr. Opin. Struct. Biol.* 19:8–13.

14. Bowie, J. U. 2005. Solving the membrane protein folding problem. *Nature.* 438:581–589.

15. Popot, J. L., and D. M. Engelman. 1990. Membrane protein folding and oligomerization: the two-stage model. *Biochemistry.* 29:4031–4037.

16. MacKenzie, K. R., J. H. Prestegard, and D. M. Engelman. 1997. A transmembrane helix dimer: structure and implications. *Science.* 276:131–133.

17. Langosch, D., B. Brosig, …, H. J. Fritz. 1996. Dimerization of the glycophorin A transmembrane segment in membranes probed with the ToxR transcription activator. *J. Mol. Biol.* 263:525–530.

18. Smith, S. O., D. Song, …, S. Aimoto. 2001. Structure of the transmembrane dimer interface of glycophorin A in membrane bilayers. *Biochemistry.* 40:6553–6558.

19. Schneider, D., and D. M. Engelman. 2004. Motifs of two small residues can assist but are not sufficient to mediate transmembrane helix interactions. *J. Mol. Biol.* 343:799–804.

20. Lemmon, M. A., J. M. Flanagan, …, D. M. Engelman. 1992. Sequence specificity in the dimerization of transmembrane $\alpha$-helices. *Biochemistry.* 31:12719–12725.

21. Doura, A. K., and K. G. Fleming. 2004. Complex interactions at the helix-helix interface stabilize the glycophorin A transmembrane dimer. *J. Mol. Biol.* 343:1487–1497.

22. Finger, C., T. Volkmer, …, D. Schneider. 2006. The stability of transmembrane helix interactions measured in a biological membrane. *J. Mol. Biol.* 358:1221–1228.

23. Anbazhagan, V., and D. Schneider. 2010. The membrane environment modulates self-association of the human GpA TM domain—implications for membrane protein folding and transmembrane signaling. *Biochim. Biophys. Acta.* 1798:1899–1907.

24. Hong, H., and J. U. Bowie. 2011. Dramatic destabilization of transmembrane helix interactions by features of natural membrane environments. *J. Am. Chem. Soc.* 133:11389–11398.

25. Fisher, L. E., D. M. Engelman, and J. N. Sturgis. 1999. Detergents modulate dimerization, but not helicity, of the glycophorin A transmembrane domain. *J. Mol. Biol.* 293:639–651.

26. Fisher, L. E., D. M. Engelman, and J. N. Sturgis. 2003. Effect of detergents on the association of the glycophorin A transmembrane helix. *Biophys. J.* 85:3097–3105.

27. Anbazhagan, V., F. Cymer, and D. Schneider. 2010. Unfolding a transmembrane helix dimer: a FRET study in mixed micelles. *Arch. Biochem. Biophys.* 495:159–164.

28. MacKenzie, K. R., and K. G. Fleming. 2008. Association energetics of membrane spanning $\alpha$-helices. *Curr. Opin. Struct. Biol.* 18:412–419.

29. Columbus, L., J. Lipfert, …, S. A. Lesley. 2009. Mixing and matching detergents for membrane protein NMR structure determination. *J. Am. Chem. Soc.* 131:7320–7326.

30. Merzlyakov, M., L. Chen, and K. Hristova. 2007. Studies of receptor tyrosine kinase transmembrane domain interactions: the EmEx-FRET method. *J. Membr. Biol.* 215:93–103.

31. Merzlyakov, M., and K. Hristova. 2008. Förster resonance energy transfer measurements of transmembrane helix dimerization energetics. *Methods Enzymol.* 450:107–127.

32. Whitmore, L., and B. A. Wallace. 2004. DICHROWEB, an online server for protein secondary structure analyses from circular dichroism spectroscopic data. *Nucleic Acids Res.* 32(Web Server issue):W668–W673.

33. Whitmore, L., and B. A. Wallace. 2008. Protein secondary structure analyses from circular dichroism spectroscopy: methods and reference databases. *Biopolymers.* 89:392–400.

34. Palladino, P., F. Rossi, and R. Ragone. 2010. Effective critical micellar concentration of a zwitterionic detergent: a fluorimetric study on *n*-dodecyl phosphocholine. *J. Fluoresc.* 20:191–196.

35. Turro, N. J., and A. Yekta. 1978. Luminescent probes for detergent solutions. A simple procedure for determination of the mean aggregation number of micelles. *J. Am. Chem. Soc.* 100:5951–5952.

36. Wolszczak, M., and J. Miller. 2002. Characterization of non-ionic surfactant aggregates by fluorometric techniques. *J. Photochem. Photobiol. Chem.* 147:45–54.

37. Kroeger, A., J. Belack, …, G. Wegner. 2006. Supramolecular structures in aqueous solutions of rigid polyelectrolytes with monovalent and divalent counterions. *Macromolecules.* 39:7098–7106.

38. Wu, P., and L. Brand. 1994. Resonance energy transfer: methods and applications. *Anal. Biochem.* 218:1–13.

39. Vitiello, G., D. Ciccarelli, …, G. D'Errico. 2009. Microstructural characterization of lysophosphatidylcholine micellar aggregates: the structural basis for their use as biomembrane mimics. *J. Colloid Interface Sci.* 336:827–833.

40. Adair, B. D., and D. M. Engelman. 1994. Glycophorin A helical transmembrane domains dimerize in phospholipid bilayers: a resonance energy transfer study. *Biochemistry.* 33:5539–5544.

41. Li, E., M. You, and K. Hristova. 2005. Sodium dodecyl sulfate-polyacrylamide gel electrophoresis and Förster resonance energy transfer suggest weak interactions between fibroblast growth factor receptor 3 (FGFR3) transmembrane domains in the absence of extracellular domains and ligands. *Biochemistry.* 44:352–360.

42. Asaoka, Y., K. Yoshida, …, Y. Nishizuka. 1993. Potential role of phospholipase A2 in HL-60 cell differentiation to macrophages induced by protein kinase C activation. *Proc. Natl. Acad. Sci. USA.* 90:4917–4921.

43. Sasaki, Y., Y. Asaoka, and Y. Nishizuka. 1993. Potentiation of diacylglycerol-induced activation of protein kinase C by lysophospholipids. Subspecies difference. *FEBS Lett.* 320:47–51.

44. Okita, M., D. C. Gaudette, …, B. J. Holub. 1997. Elevated levels and altered fatty acid composition of plasma lysophosphatidylcholine (lysoPC) in ovarian cancer patients. *Int. J. Cancer.* 71:31–34.

45. Taylor, L. A., J. Arends, …, U. Massing. 2007. Plasma lyso-phosphatidylcholine concentration is decreased in cancer patients with weight loss and activated inflammatory status. *Lipids Health Dis.* 6:17.

46. Skipski, V. P., M. Barclay, …, F. M. Archibald. 1967. Lipid composition of human serum lipoproteins. *Biochem. J.* 104:340–352.

47. Lee, A. G. 2003. Lipid-protein interactions in biological membranes: a structural perspective. *Biochim. Biophys. Acta.* 1612:1–40.

48. Nyholm, T. K., S. Ozdirekcan, and J. A. Killian. 2007. How protein transmembrane segments sense the lipid environment. *Biochemistry.* 46:1457–1465.

49. Huang, H. W. 1986. Deformation free energy of bilayer membrane and its effect on gramicidin channel lifetime. *Biophys. J.* 50:1061–1070.

50. Mineev, K. S., E. V. Bocharov, …, A. S. Arseniev. 2011. Dimeric structure of the transmembrane domain of glycophorin a in lipidic and detergent environments. *Acta Naturae.* 3:90–98.